Short communication

Structural changes of a Li/S rechargeable cell in Lithium Metal Polymer technology

CrossMark

Margaud Lécuyer [a,b], Joël Gaubicher [b,*], Marc Deschamps [a], Bernard Lestriez [b], Thierry Brousse [b], Dominique Guyomard [b]

[a] Batscap, Odet, Ergué Gabéric, 29556 Quimper Cedex 9, France
[b] Institut des Matériaux Jean Rouxel, CNRS/UMR 6502, 2 rue de la Houssinière, BP 32229, 44322 Nantes Cedex 3, France

HIGHLIGHTS

- Morphological changes in Li/S batteries with polymer electrolyte.
- Capacity fading between the first two cycles.
- Cathode's collapse during the first discharge.
- Negative influence of polysulfides diffusion on long-term cyclability.
- Precipitation of Li_2S/Li_2S_2 on lithium anode after several cycles.

ARTICLE INFO

ABSTRACT

Lithium/sulfur batteries in Lithium Metal Polymer (LMP) technology suffer from poor reversibility and important capacity fade. In this paper we studied structural evolutions of Li/S cells with PEO-based (poly(ethylene oxide)) dry polymer electrolyte, by means of scanning electron microscopy (SEM) and energy-dispersive X-ray spectroscopy (EDX). Discharge occurs along with dissolution of the active material into soluble polysulfides in PEO. Diffusion of the sulfide species results in important volume changes of both the electrode and the electrolyte. This eventually leads to collapse of the electrode upon a few cycles, which contributes to the poor cyclability of the battery. In order to prevent this phenomenon, the mechanical strength of the cathode was enhanced by adding poly(vinylidene fluoride) (PVDF) in its composition. However, although PVDF helps maintaining the electrode's structure, it could not completely solve the cyclability issue.

1. Introduction

Environmental issues such as global warming and atmospheric pollution are just so many reasons to the fast development of many kinds of rechargeable batteries with high energy-density. Issues relate to the development of low-cost batteries with high autonomy that could take place into electric vehicles (EVs) to progressively replace the combustion engines vehicle fleet. Li/S batteries could meet these expectations because sulfur is cheap and shows very high specific capacity (1675 mAh/g$_{sulfur}$) and energy density (2600 Wh/kg$_{sulfur}$), assuming complete reduction into lithium sulfide Li_2S near 2 V [1].

However, serious challenges of two kinds remain to be addressed before commercial applications could emerge. The first one is related to difficulties in reaching complete utilization of its impressive capacity [2–6] because of both its electronic and ionic insulating nature [7,8]. Moreover, these properties make the addition of relatively large amounts of conductive materials mandatory, which limits the overall electrode weight and volumetric capacities. The second and main issue relates to capacity retention on cycling. It lies in the specific discharge mechanism of Li/S battery, much different from intercalation–de-intercalation reactions taking place in commercial lithium-ion batteries [9]. As a matter of fact, molecular sulfur rings S_8 are progressively reduced into intermediate lithium polysulfides Li_2S_n ($n \geq 4$) [10], that are highly soluble in

* Corresponding author. Tel.: +33 2 40 37 39 27/63 22; fax: +33 2 40 37 39 95.
 E-mail addresses: joel.gaubicher@cnrs-imn.fr, j.gaubicher@gmail.com (J. Gaubicher).

common organic electrolytes such as glyme ethers [4,11] or 1,3-dioxolane [2,7] but also in polymer electrolytes such as PEO [1].

Consequences of polysulfides' diffusion are controversial. Some teams try to prevent polysulfides diffusion by using charged polymers such as Nafion® [12,13] or by enhancing sulfur interactions with carbon black [5,14–16], while others get good results by protecting the lithium anode [17] but do not prevent the active material from diffusing. Nevertheless, some of the highly soluble polysulfides are being reduced into insoluble Li_2S upon contact with lithium, and the others, being far from the cathode, are responsible for the poor recharge kinetics as they must diffuse back through the electrolyte to be reduced inside the cathode. Therefore, the polysulfides diffusion leads to partial reversibility and causes poor capacity retention. Few studies only have been conducted in respect of LMP based Li/S batteries. As a matter of fact, dry PEO has been already proposed as a binder both in the cathode and electrolyte but revealed poor cyclability [1,18]. In this study, our goal is to pinpoint issues related to LMP sulfur-based battery. In particular, we describe the correlation between the evolution of both the electrode and the dry PEO based electrolyte structures with the fast capacity fade observed during the first cycles. Processes governing capacity retention will be discussed based on SEM and EDX post-mortem analyses.

Finally, we investigated the effect of the addition of a structuring binder such as PVDF into the composition of the sulfur-electrode. Impact on morphological evolution of the positive electrode as well as on the electrochemical performances will be reported.

2. Experimental section

2.1. Preparation of composite sulfur cathode

Carbon black (Ketjenblack®), tri-hydrated lithium perchlorate $LiClO_4·3(H_2O)$ (Aldrich), poly(ethylene oxide-co-butylene oxide) polymer (HQSEB, Nippon Shokubai) and sulfur powder (Aldrich, Sublimed sulphur), at weight ratios of 5:9:32:54 were mixed in water and then introduced in a plastograph® Brabender® at 80 °C and 80 rpm for 20 min. Then, the paste was spread between two heating-rolls (95 °C) over an aluminum current-collector, coated with carbon. Water was evaporated in an oven for 20 min at 105 °C.

The electrodes containing PVDF were prepared following the same method but replacing a part of HQSEB by PVDF and using LiTFSI (provided by 3 M) as the lithium salt and propylene carbonate as the solvent. They were dried at 80 °C under vacuum during 1 h. These cathodes are named by the percentage of PVDF in the total of polymer.

2.2. Cell assembly

PEO-based electrolytes as well as lithium foils were provided by Batscap. The cells were assembled in a dry room under controlled moisture (dew point: −55 °C) by stacking lithium, electrolyte and sulfur cathode on an aluminum current-collector at 80 °C. On the negative side, the current collector was a copper foil hand-welded to lithium. Both current-collectors were welded by ultrasound to copper-connectors. Cells were air tight sealed in coffee-bags and vacuumed in order to avoid air pockets.

2.3. Measurements

The charge and discharge performances of the cells were measured galvanostatically at different rates with a Bitrode battery cell testing system at 100 °C. After cycling, cells' morphologies were investigated by SEM (Hitachi Analytical TableTop Microscope TM3000). EDX measurements were carried out using an Oxford

Instrument X-ray Microanalysis, with a resolution of about 1 μm³, (acquisition time: 30 s). The calibration was verified on fluorine content in the electrolyte. Initial thicknesses of electrolytes were measured with a Mitutoyo sensor (sensibility: 0.5 μm).

3. Results and discussion

3.1. Morphological evolution of the PEO-based Li/S battery during the first cycle

The typical voltage profile of the Li/S battery containing a copolymer of PEO as the polymer both in the electrolyte and the cathode is displayed on Fig. 1. The discharge process can be divided into two main regions, although a third sloping plateau is visible. As previously described in the literature [19], these two main regions correspond to two stages of the discharge mechanism. In the first step, between 2.8 and 2.1 V, elementary sulfur S_8 is reduced into long-chain polysulfides Li_2S_8. At lower voltages, long-chain polysulfides are progressively reduced into shorter-chain polysulfides Li_2S_n, with $1 \leq n < 8$.

As suggested by the complex mechanism of discharge depicted for Li/S batteries, huge volume variations can be expected to occur inside the positive electrode when active material solubilizes into the polymer matrix of both the electrode and electrolyte. In order to describe morphology changes of a LMP Li/S battery and to understand its consequences on cyclability, we performed structural analysis by SEM. These observations were made at different depths of discharge, as depicted on the voltage profile on Fig. 1.

Before SEM observations, the cell was removed from its coffee-bag under controlled moisture (dew point −55 °C). A piece of the cell was cut with a blade, frozen in liquid nitrogen and sliced with a microtome to get a proper cross-section. Cross-sections are displayed on Fig. 2. Thicknesses are deliberately not indicated in the SEM images. Prior to discharge, sulfur particles of about 2–20 μm are well dispersed in the carbon/polymer matrix (Fig. 2a). Moreover, the initial poor adhesion at the interface cathode/electrolyte that can be seen here (Fig. 2a) is not expected to be limiting while cycling. From the beginning of discharge, these particles dissolve and none remain visible at 2.35 V (Fig. 2d). At this depth of discharge, the cathode's integrity looks preserved. At deeper depths of discharge, large voids appear in the cathode (Fig. 2e). Their formation is ascribable to polysulfides dissolution and diffusion (see below), resulting by the way to the ripping of the polymer walls when they are no more maintained by the presence of the active
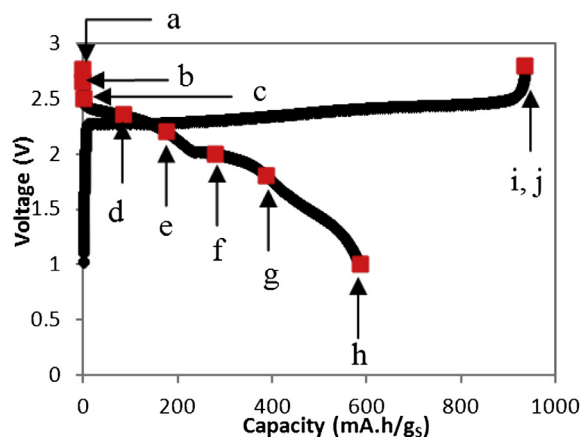

Fig. 1. Typical discharge and charge profiles of the Li/S cell. Electrodes were recovered after partial discharges and charges indicated by a to j, for further analysis.
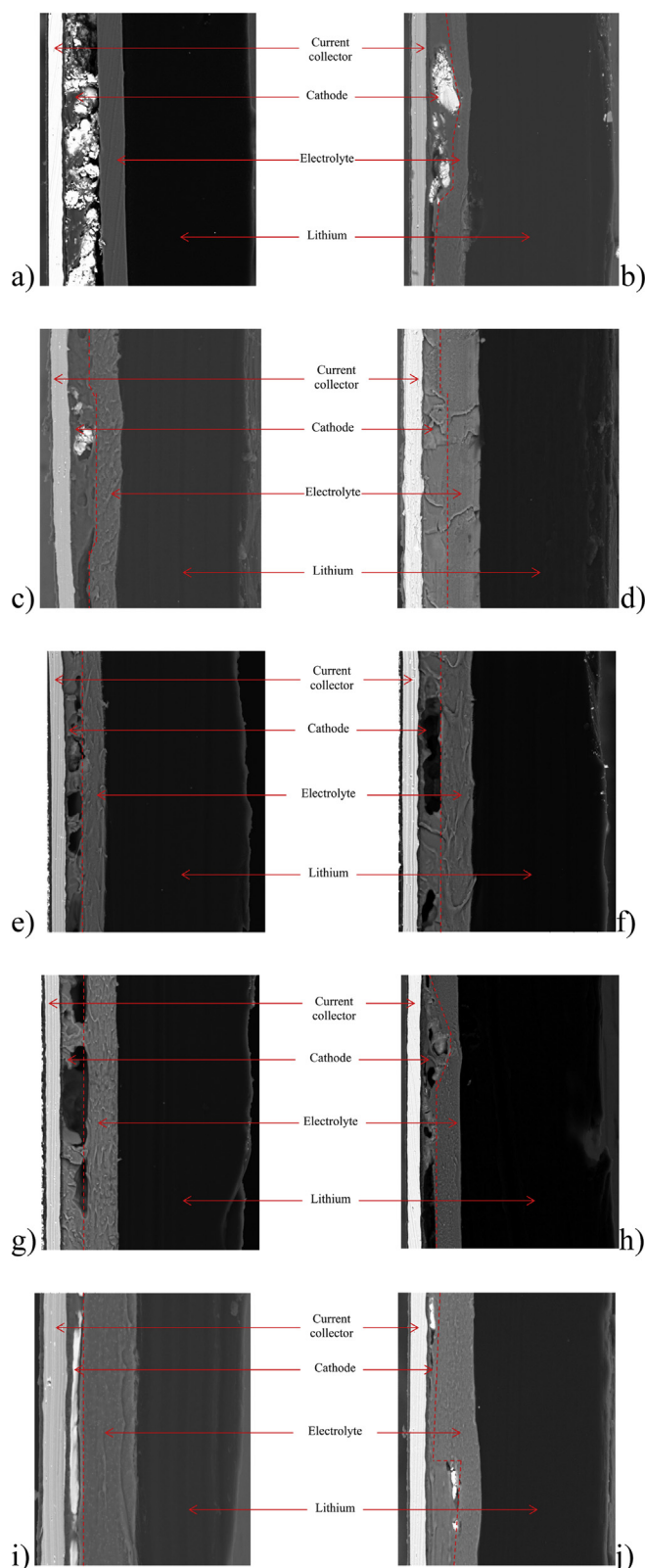
Fig. 3. Swelling of the electrolyte, represented by the ratio between the final volume measured by SEM on the initial volume of the electrolyte and S content in the bulk of electrolyte, measured by EDX.

material. Although the cell's structure do not evolve much until the end of discharge, the cathode collapses because of the diffusion of active material out of the electrode. As a matter of fact, the thickness of the electrolyte increases by 32% whereas that of the cathode is reduced by 68% (Figs. 2h and 3).

At the end of discharge (Fig. 2h), Li_2S and/or Li_2S_2 precipitate(s) inside remaining voids. The latter are easily identified by their instantaneous reaction with the electron beam. These analyses illustrate the possibility of a complete reduction of sulfur species in contact with the cathode.

During the subsequent charge, atomic sulfur is reformed (Fig. 2i and j). But, as previously noticed, the cathode's structure has changed during first discharge. Consequently, sulfur forms at the surface of the holes that have not collapsed during the previous discharge, resulting in the formation of non-dispersed agglomerates in place of the initial smaller grains (see Fig. 2a, i and j). This results in poor dispersion of active material in the polymer matrix and to important variability in the electrode's thickness. As a consequence, the electrode's structure will never be the same as pristine's.

Fig. 2. SEM images of the evolution of the morphology of the battery along the first cycle: cross-section views; a) before discharge, b) discharged at 2.65 V, c) discharged at 2.50 V, d) discharged at 2.35 V, e) discharged at 2.2 V, f) discharged at 2 V, g) discharged at 1.8 V, h) discharged at 1 V, i) and j) charged at 2.8 V.
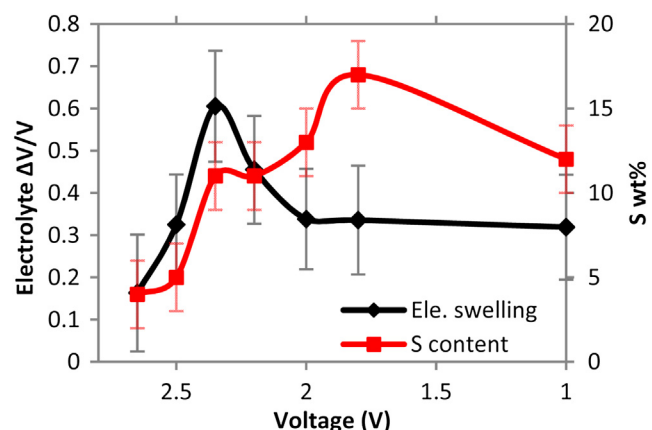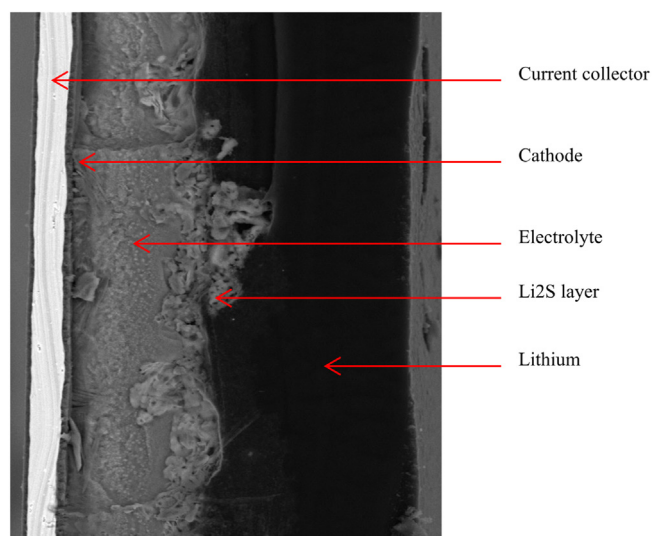

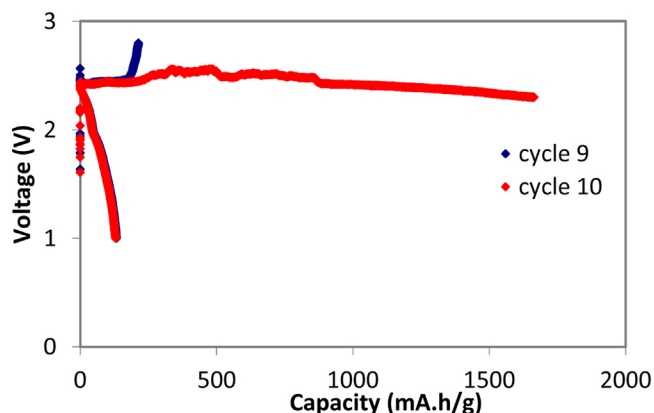**Fig. 4.** Cross-sections SEM image of a Li/S cell after 11 cycles.

Fig. 5. Voltage profiles of the 9th and 10th cycles of a Li/S cell at D/10.

These observations highlight the issue related to the collapse of the sulfur-based electrode, and point out polysulfides dissolution and diffusion as the main causes for this loss of structural integrity. In order to be able to quantify the diffusion of active material in the cell by EDX measurements, $LiClO_4$ was used as lithium salt rather than LiTFSI that contains sulfur atoms. At every point indicated on the voltage profile (Fig. 1), sulfur content in the bulk of the electrolyte was determined by EDX measurements in the bulk of the electrolyte (Fig. 3).

During the first cycle, more and more sulfur atoms are detected in the bulk of electrolyte as the discharge goes deeper down to 1.8 V (Fig. 3, red curve in the web version), revealing the dissolution of polysulfides in the PEO copolymer and their diffusion through the cell. Note that if all the sulfur was homogeneously dissolved in the cathode and the electrolyte, the S content would be around 22 wt%. A great part of the active material has consequently diffused during the first discharge. At the end of discharge, as Li_2S precipitates, the S content decreases in the bulk of the electrolyte. The variation of the electrolyte volume is also reported on Fig. 3 (black curve) along with that of the S content in the electrolyte. The evolution of the electrolyte swelling is readily ascribed to the quantity of dissolved polysulfides but it may also be linked with their nature. This is under further investigations. At the end of discharge, precipitation of Li_2S_2 and/or Li_2S inside the cathode is likely to occur along with diffusion of soluble polysulfides back to the positive electrode. As a matter of fact, the electrolyte's thickness decreases at the end of the discharge.

During the first charge, all dissolved sulfide species are expected to be re-oxidized at the surface of the cathode in order to re-form atomic sulfur. However, more than 5 wt% of sulfur was detected in the electrolyte at the end of the charge, revealing the presence of remaining dissolved polysulfides. This is another reason for the loss of capacity after the first discharge: some of the active material is no more available.

To summarize, the first cycle of a LMP Li/S cell is accompanied by a loss of structure of the positive electrode and a loss of the dispersion of the active material in the polymer matrix. Moreover, some sulfur irreversibly dissolves in the cell under the form of polysulfides that remain in the electrolyte at the end of the charge, instead of precipitating inside the cathode. Both of these phenomena contribute to the huge capacity fading between the first two cycles.

3.2. Morphological evolution of the PEO-based Li/S battery during the subsequent cycles

Since the first cycle, an accumulation of sulfur species progressively takes place at the lithium interface (not shown), most likely due to the reduction of polysulfides into Li_2S upon contact with lithium. This presumably traps irreversibly active material and
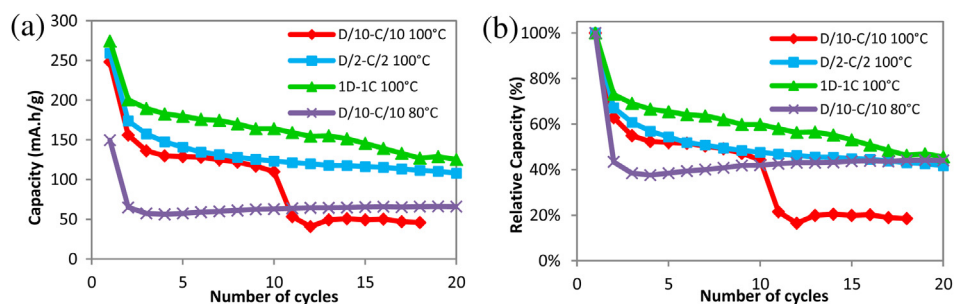

Fig. 6. Evolution of the discharged gravimetric (a) and relative (b) capacities on cycling for different cycling rates and temperatures. The relative capacity corresponds to the ratio of the discharged capacity at cycle *n* by that at cycle 1.
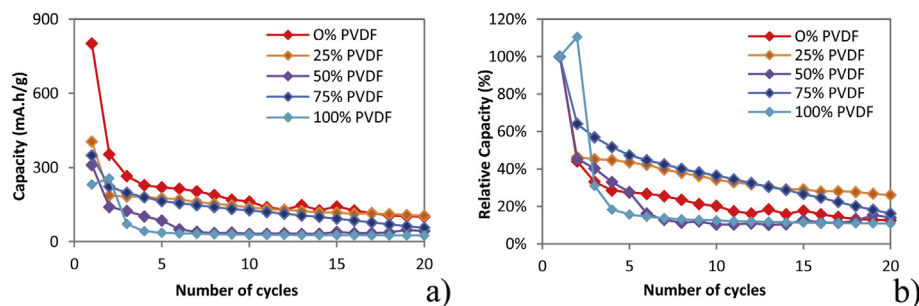

Fig. 7. Evolution of the discharged gravimetric capacity (a) and of the relative capacity (b) on cycling, for different PVDF contents. The relative capacity corresponds to the ratio of the discharged capacity at cycle *n* by that at cycle 1.

causes additional capacity loss. After some cycles, a thick layer of Li$_2$S is observed at the lithium/electrolyte interface (Fig. 4).

This insulating layer leads to difficulties to re-charge the Li/S cell. No sulfur precipitation is visible in the cathode (Fig. 4) while the charge capacity increases continuously with a charge potential limited to 2.6 V (Fig. 5, red curve) instead of reaching 2.8 V (Fig. 5, blue curve). The current through the cell may be ascribed to parasitic reactions such as shuttle mechanism and does not contribute to sulfur species re-oxidation. No real charge happens, which is related to a sharp decrease of coulombic efficiency from 62% to 8% between the 9th and the 10th cycles. The formation of such a huge Li$_2$S interphase between electrolyte and lithium always matches with an important discharge capacity fading as the one on Fig. 5 (red curve in the web version) between the 10th and the 11th discharges.

Consequently, these observations highlight that polysulfides diffusion is detrimental to the Li/S cell cyclability as it results in a loss of active material being trapped at the lithium/electrolyte interface.

3.3. Overview of parameters influencing the cyclability of Li/S cells

As shown previously, the evolution of morphology of the Li/S cell and the diffusion of active material during the first cycle result in an important loss of capacity (Fig. 6, red curve in the web version). Fig. 6 summarizes the influence of cycling rate and temperature on the discharged capacity. Initial capacities appear to be quite similar at 100 °C irrespective of the cycling rate (Fig. 6a). Capacity fading is however less pronounced when the cycling rate increases (Fig. 6b) which may be correlated with the time constant for polysulfides diffusion through the cell.

As expected, temperature strongly influences discharged capacity (Fig. 6a) as ionic conductivity of electrolyte is thermally activated. At 80 °C (Fig. 6b), an important loss of capacity is noticeable between the first and the second cycles and can be ascribed to the collapse of the cathode. However, from the 2nd cycle, the capacity remains stable and even increases until the 20th cycle. Further structural investigations are presently performed to explain the lower fading observed at 100 °C vs. 80 °C. Moreover, a dramatic loss of capacity occurs at 100 °C (here at the 10th cycle), but it has not been noticed at 80 °C. As diffusion phenomena at lower temperatures are slowed down, the stabilization of capacity at 80 °C supports our hypothesis that polysulfides' diffusion alters Li/S cell's cyclability.

3.4. Reinforcement of mechanical strength of the sulfur cathode by addition of PVDF

Previous correlation between cathode collapsing and capacity loss on first cycle leads us to search for mechanical reinforcement of sulfur-based cathode. In this aim PVDF was added in the composition of electrodes. Indeed, PVDF presents a higher Young modulus 1.5 GPa [20] than PEO: 0.29 GPa [21] at room temperature.

According to results shown on Fig. 7a, the introduction of PVDF strongly influences the initial discharged capacity: as for the first cycle, the higher the PVDF content, the lower the discharge capacity. This result can be ascribed to poor ionic conductivity of this polymer. On contrary, on the second cycle, the higher the PVDF content, the lower the capacity fading (Fig. 7b). To understand this tendency, SEM observations were performed after the first discharge and the first cycle allowing to follow the evolution of cathode's morphology (Fig. 8). First, it appears that the introduction of PVDF in the cathode composition results in a better dispersion of sulfur grains in the polymer matrix. This effect could be ascribed to the higher viscosity of the PVDF which produces smaller sulfur
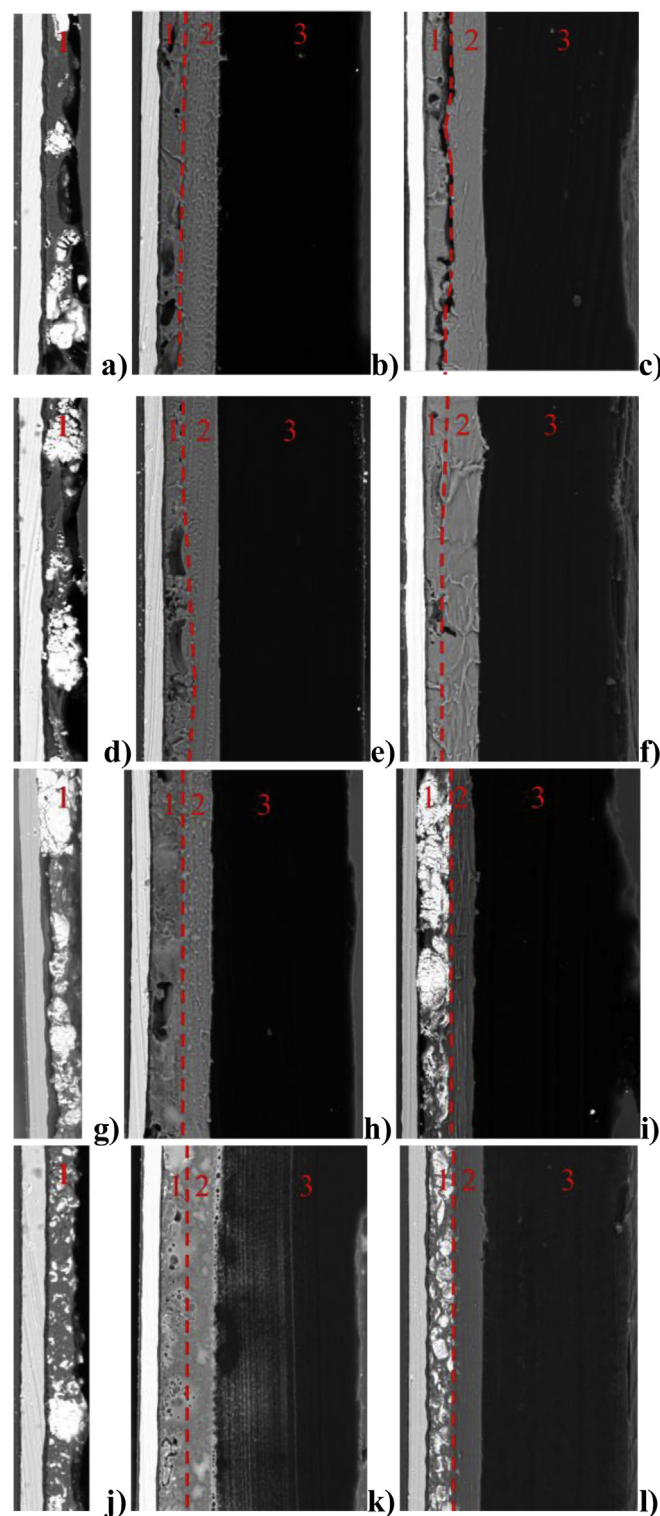

Fig. 8. SEM images of the cathode in initial state (left column) and of a Li/S cell containing PVDF in the cathode composition after 1 discharge (middle column) and 1 cycle (right column) at D/10-C/10. Layer 1: cathode (zoomed); layer 2: electrolyte; layer 3: lithium foil. a) b) c) 25% PVDF; d) e) f) 50% PVDF; g) h) i) 75% PVDF; j) k) l) 100% PVDF.

nodules thus preventing re-agglomeration of sulfur particles. Second, the higher the PVDF content, the smaller the holes in the cathode after the first discharge and, as a result, the more preserved the structure after the first cycle. Similarly, larger PVDF contents result in smoother cathode/electrolyte interface after one cycle and

in the precipitation of sulfur in smaller grains. This observation highlights the correlation between capacity retention at the second discharge and conservation of the cathode's structure. Moreover, sulfur re-precipitation is clearly observed upon charge when PVDF content is higher than 50% (Fig. 8i, l). This might be ascribed to the low solubility of polysulfides in this polymer that would therefore limit their dissolution in the polymer matrix and favor sulfur precipitation.

Therefore results suggest that the introduction of PVDF in cathode's composition decreases capacity fading between the first two cycles by enhancing the mechanical resiliency of the cathode. The adverse effect is however a decrease of the electrode reactivity presumably associated with a lower ionic conductivity. Nevertheless, it is clear that optimizing the mechanical strength of the cathode cannot fully address the cyclability issue, therefore highlighting the necessity to prevent polysulfides diffusion away from the cathode.

4. Conclusion

In this work, we characterized the evolution of morphology of a Li/S cell with a dry polymer electrolyte by SEM observations and EDX measurements. Results revealed a collapse of the cathode during the first cycle and a complete loss of its pristine structure. In parallel, the polymer electrolyte swells because of dissolution and diffusion of polysulfides. At the end of discharge, Li_2S_2 and/or Li_2S precipitate(s) inside the electrode. During the subsequent charge, large aggregates of sulfur are formed, and the initial morphology of the electrode is not recovered. Moreover, some polysulfides remain dissolved in the electrolyte and a layer of Li_2S forms at the Li/electrolyte interface. This layer can become very thick after a tens of cycles and leads to a blocking of the re-charge of the cell and by the way, to a severe loss of capacity.

Our experiments showed that increasing the cycling rate or decreasing the cycling temperature improved cyclability, revealing the negative influence of polysulfides diffusion in the cell.

In order to increase the mechanical strength of the positive electrode, PVDF was added to its composition. This resulted in lower initial discharged capacities as the PVDF ratio increased and in lower capacity fading between the first two discharges. This was ascribed to the conservation of the electrode's structure. However, the low capacity retention at following cycles proves the importance of controlling polysulfides diffusion through the cell.

To conclude, these results show that it is important to maintain the initial structure of the cell to get a good cyclability. To this purpose, two ways must be coupled: the first one is to enhance the mechanical strength of the cathode; the second one is to prevent polysulfides diffusion that gives rise to both huge cell volume variations and Li_2S passivation layer deposition at the lithium electrode.

References

[1] D. Marmorstein, T.H. Yu, K.A. Striebel, F.R. McLarnon, J. Hou, E.J. Cairns, J. Power Sources 89 (2000) 219–226.
[2] R.D. Rauh, K.M. Abraham, G.F. Pearson, J.K. Surprenant, S.B. Brummer 126 (4) (1979) 523–527.
[3] P. Leghié, J.P. Lelieur, E. Levillain, Electrochem. Commun. 4 (2002) 406–411.
[4] S.E. Cheon, K.S. Ko, J.H. Cho, S.W. Kim, E.Y. Chin, H.T. Kim, J. Electrochem. Soc. 150 (6) (2003) A796–A799.
[5] X. Ji, K.T. Lee, L.F. Nazar, Nat. Mater. 8 (2009) 500–506.
[6] Y.V. Mikhaylik, J.R. Akridge, J. Electrochem. Soc. 151 (11) (2004) A1969–A1976.
[7] E. Peled, Y. Sternberg, A. Gorenshtein, Y. Lavi, J. Electrochem. Soc. 136 (1989) 1621–1625.
[8] J.A. Dean, Lange's Handbook of Chemistry, third ed., McGraw-Hill, New York, 1985, pp. 3–5.
[9] M. Armand, J.M. Tarascon, Nature 451 (2008) 652–657.
[10] J. Shim, K.A. Striebel, E.J. Cairns, J. Electrochem. Soc. 149 (2002) A1321–A1325.
[11] Y.S. Nimon, M.Y. Chu, S.J. Visco, 6 017 651 US, January 2000.
[12] Z. Jin, K. Xie, X. Hong, Z. Hu, X. Liu, J. Power Sources 218 (2012) 163–167.
[13] Y. Cao, X. Li, I.A. Aksay, J. Lemmon, Z. Nie, Z. Yang, J. Liu, Phys. Chem. Chem. Phys. 13 (2011) 7660–7665.
[14] J.Z. Wang, L. Lu, M. Choucair, J.A. Stride, X. Xu, H.K. Liu, J. Power Sources 196 (2011) 7030–7034.
[15] G. Zheng, Y. Yang, J.J. Cha, S.S. Hong, Y. Cui, Nano. Lett. 11 (2011) 4462–4467.
[16] B. Zhang, X. Qin, G.R. Li, X.P. Gao, Energy Environ. Sci. 3 (2010) 1531–1537.
[17] Y.M. Lee, N.S. Choi, J.H. Park, J.K. Park, J. Power Sources 119-121 (2003) 964–972.
[18] S.S. Jeong, Y.T. Lim, Y.J. Choi, G.B. Cho, K.W. Kim, H.J. Ahn, K.K. Cho, J. Power Sources 174 (2007) 745–750.
[19] V.S. Kolosnitsyn, E.V. Karaseva, Russ. J. Electrochem. 44 (5) (2008) 506–509.
[20] http://www.engineeringtoolbox.com/physical-properties-thermoplastics-d_808.html.
[21] L.M. Bellan, J. Kameoka, H.G. Craighead, Nanotechnology 16 (2005) 1095–1099.